ANESTHESIOLOGY

Isoflurane Exposure in Juvenile *Caenorhabditis elegans* Causes Persistent Changes in Neuron Dynamics

Gregory S. Wirak, B.S., Christopher V. Gabel, Ph.D., Christopher W. Connor, M.D., Ph.D.

Anesthesiology 2020; 133:569–82

EDITOR'S PERSPECTIVE

What We Already Know about This Topic

- Experimental data in laboratory animals demonstrate that early life exposure to anesthetics can induce lasting neurobehavioral and cognitive alterations
- The neurobiological bases of these alterations are incompletely understood
- *Caenorhabditis elegans* is a well suited experimental model for long-term functional imaging of neurons after anesthesia exposure

What This Article Tells Us That Is New

- Exposure of *Caenorhabditis elegans* to isoflurane for 3 h during the first larval stage results in lifelong attenuation in spontaneous crawling reversal behavior
- These effects correlate with persistently altered activity dynamics of command interneurons mediating crawling reversals
- Genetic dissection of potential underlying mechanisms reveals that these effects are modulated by a loss of *daf-16* or mechanistic Target of Rapamycin (mTOR) activity, consistent with a persistent pathologic activation of stress-response pathways

ABSTRACT

Background: Animal studies demonstrate that anesthetic exposure during neurodevelopment can lead to persistent behavioral impairment. The changes in neuronal function underlying these effects are incompletely understood. *Caenorhabditis elegans* is well suited for functional imaging of postanesthetic effects on neuronal activity. This study aimed to examine such effects within the neurocircuitry underlying *C. elegans* locomotion.

Methods: *C. elegans* were exposed to 8% isoflurane for 3 h during the neurodevelopmentally critical L1 larval stage. Locomotion was assessed during early and late adulthood. Spontaneous activity was measured within the locomotion command interneuron circuitry using confocal and light-sheet microscopy of the calcium-sensitive fluorophore GCaMP6s.

Results: *C. elegans* exposed to isoflurane demonstrated attenuation in spontaneous reversal behavior, persisting throughout the animal's lifespan (reversals/min: untreated early adulthood, 1.14 ± 0.42, *vs.* isoflurane-exposed early adulthood, 0.83 ± 0.55; untreated late adulthood, 1.75 ± 0.64, *vs.* isoflurane-exposed late adulthood, 1.14 ± 0.68; $P = 0.001$ and 0.006, respectively; $n > 50$ animal tracks/condition). Likewise, isoflurane exposure altered activity dynamics in the command interneuron AVA, which mediates crawling reversals. The rate at which AVA transitions between activity states was found to be increased. These anesthetic-induced effects were more pronounced with age (off-to-on activity state transition time (s): untreated early adulthood, 2.5 ± 1.2, *vs.* isoflurane-exposed early adulthood, 1.9 ± 1.3; untreated late adulthood, 4.6 ± 3.0, *vs.* isoflurane-exposed late adulthood, 3.0 ± 2.4; $P = 0.028$ and 0.008, respectively; $n > 35$ traces acquired from more than 15 animals/condition). Comparable effects were observed throughout the command interneuron circuitry, indicating that isoflurane exposure alters transition rates between behavioral crawling states of the system overall. These effects were modulated by loss-of-function mutations within the FoxO transcription factor *daf-16* and by rapamycin-mediated mechanistic Target of Rapamycin (mTOR) inhibition.

Conclusions: Altered locomotive behavior and activity dynamics indicate a persistent effect on interneuron dynamics and circuit function in *C. elegans* after developmental exposure to isoflurane. These effects are modulated by a loss of *daf-16* or mTOR activity, consistent with a pathologic activation of stress-response pathways.

(Anesthesiology 2020; 133:569–82)

Rodent and primate studies suggest that early exposure to volatile anesthetics can be neurotoxic, producing lasting impairments in learning and memory acquisition.[1–3] Primate studies further provide evidence for the impact of anesthesia on socioemotional development.[4,5] Although persistent anesthesia-induced neurobehavioral alterations do not appear to be clinically prevalent among singly exposed patients,[6–9] rare yet potentially high-risk populations cannot be identified without a mechanistic understanding of these effects.

The nematode *Caenorhabditis elegans* also exhibits persistent behavioral changes after volatile anesthetic exposure during development. Because *C. elegans* lacks a cardiovascular system, these changes cannot be related to perturbations of cerebral perfusion as might be implicated in mammals.

This article is featured in "This Month in Anesthesiology," page 1A. This article is accompanied by an editorial on p. 495. This article has a visual abstract available in the online version. Part of the work presented in this article has been presented at the Post Graduate Assembly in Anesthesiology (PGA72) in New York, New York, December 7–11, 2018.

Submitted for publication December 10, 2019. Accepted for publication April 2, 2020. Published online first on May 21, 2020. From the Department of Physiology and Biophysics, Boston University School of Medicine, Boston, Massachusetts (G.S.W., C.V.G., C.W.C.); and the Department of Anesthesiology, Perioperative and Pain Medicine, Brigham and Women's Hospital, Boston, Massachusetts (C.W.C.).

 Anesthesiology 2020; 133:569–82. DOI: 10.1097/ALN.0000000000003335

<zdoi;. DOI: 10.1097/ALN.0000000000003335>

Gentry *et al.*[10] showed that larvae exposed to volatile anesthetics demonstrate deficits in their ability as adults to perform chemotaxis: the behavioral strategy for searching for food. This abnormality was exclusively observed in worms exposed during a narrow developmental window, the L1 larval stage. Chemotaxis is a complex behavior relying on chemosensation and modulation of behavioral crawling states. It is one of the subtler yet essential integrative tasks performed by the organism.[11]

C. elegans depends upon the stochastic nature of its locomotion to effectively chemotax. Its movement can be described as a random walk, facilitating dispersion throughout its environment.[12,13] Locomotion consists of constant forward movement interrupted by sharp, randomized changes in its direction of movement ("pirouettes"). Chemotaxis is accomplished by modulating the frequency of these pirouettes as the animal nears a food source.[14] Bouts of spontaneous backward movement ("reversals"), which interrupt the worm's otherwise forward movement, initiate pirouettes and are critical to effective chemotaxis.[15,16] The neurocircuitry underlying this behavior is well studied and exhibits a bimodal pattern of excitation, corresponding to either forward or backward movement states.[17,18] Although sensory input modulates the state of this network, it also switches between states spontaneously, eliciting the observed intermittent reversal behavior. Here we examine persistent effects on this network function after developmental exposure to isoflurane, using functional neuronal imaging in *C. elegans* to demonstrate a mechanistic neuronal correlate to the previously described behavioral deficits.

Materials and Methods

C. elegans Strains

The animals were maintained at 20°C on nematode growth medium–agarose plates coated with *Escherichia coli* OP50. When specified, nematode growth medium plates contained 100 μM rapamycin (LC Laboratories, USA), initially dissolved in dimethyl sulfoxide to a concentration of 0.1%. The experiments were performed using hermaphrodites cultured to either early or late adulthood (2 and 10 days after the L1 larval stage, respectively). Imaging experiments were performed using the transgenic strain QW1574 (*lite-1[ce314], zfis146[nmr-1::NLSwCherry::SL2::GCaMP6s, lim-4(−3328–2174)::NLSwCherry::SL2::GCaMP6s, lgc-55(−120–773)::NLSwCherry::SL2::GCaMP6s, npr-9::NLSwCherry::SL2::GCaMP6s] #18.9* [from *zfex696*]), which expresses cytoplasmic calcium-sensitive green fluorescent protein GCaMP6s and a nuclear-localized red fluorescent protein NLSwCherry in eight pairs of premotor interneurons (AVA, AVB, AVD, AVE, AIB, RIM, RIV, and PVC) on an otherwise unmodified wild-type N2 background. When specified, imaging experiments were performed using QW1574 worms that had been crossed with the following mutant strains: MT6347 (*ced-3[n2433]*), which harbors a missense mutation within *ced-3*, a key mediator of the apoptotic pathway; CB1370 (*daf-2[e1370]*), which harbors a temperature-sensitive mutation within the *C. elegans* insulin/insulin-like growth factor 1 receptor ortholog *daf-2*; or CF1038 (*daf-16[mu86]*), which harbors a suppressive mutation within the FoxO transcription factor *daf-16*. Behavioral experiments were performed with QW1574 as above. The QW1574 strain was generated in the laboratory of Dr. Mark Alkema (University of Massachusetts Medical School, Worcester, Massachusetts), and MT6347, CB1370, and CF1038 were obtained from the Caenorhabditis Genetics Center (University of Minnesota, Minneapolis, Minnesota). Invertebrate research, such as that involving *C. elegans*, is exempt from institutional animal care and use committee review, as specified by the Animal Welfare Act and the Health Research Extension Act.

Anesthesia

Gravid adults were transferred to fresh nematode growth medium–agarose plates (with 100 μM rapamycin, when specified) and allowed to lay eggs for a period of 2 h. The adults were then removed, and the eggs were allowed to hatch. 15 h after the timed egg laying, half of the newly hatched L1-stage larvae were exposed to an atmosphere of 8% isoflurane in room air (19 to 22°C) for a period of 3 h as previously described,[19] while the other half were maintained in an adjacent, matched environment under room air only. The anesthetized animals were recovered to room air. These colonies were then maintained in the laboratory for monitoring and assessment for either a further 2 days, (*i.e.*, to early adulthood, 1 day after the larval stage) or for a further 10 days (*i.e.*, to late adulthood, 9 days after the larval stage). The animals hatched on rapamycin-containing plates were maintained on these same plates throughout their development.

Behavioral Assays

Anterior Touch Responsiveness

The worms were stroked with an eyelash across the anterior portions of their body while engaging in forward locomotion in a food-free environment. Individual animals were stroked 5 times, with an interval of at least 5 min between stimuli. The animals were scored as responsive or nonresponsive to each stimulus depending on whether they initiated a movement reversal or not, by an experimenter blind to condition. The anterior touch responsiveness assay was performed during late adulthood.

Spontaneous Reversal Rate

The worms were observed freely moving in an environment devoid of food. The animals were transferred to a clear agar dish and allowed to rest for 15 min, after which their crawling movement was video recorded. The movies

were analyzed by an experimenter blind to condition using ImageJ[20] to count the number of spontaneous reversals the animals initiated over a given period of time (between 2 and 10 min). The spontaneous reversal rate was assessed during early and late adulthood.

Confocal Imaging

Before imaging, the worms were encased in a polyethylene glycol hydrogel after a brief exposure to 5 mM tetramisole. The hydrogel provides an effective method of restricting the mobility of the worms[21] without exposing them to additional and potentially confounding pharmacologic agents. Within the completely mapped neurocircuitry of *C. elegans*, the AVA and AVB neurons are well characterized as mediating reverse and forward crawling, respectively, representing the two major behavioral states of the system.[17] Spontaneous *in vivo* neuronal activity was assessed in the command interneuron AVA using confocal laser fluorescence microscopy and the calcium indicator GCaMP6s, as previously described.[19] Image sequences were acquired for 10 min for each worm at a rate of 4 images/s. The acquired time-lapse images were analyzed by identifying and tracking the nucleus of the AVA neuron in the red fluorescent signal (as described above for the QW1574 strain) and then extracting the green GCaMP fluorescence intensity in the surrounding soma of the identified neuron. The animals were imaged during early and late adulthood.

Light-sheet Imaging

As above, the worms were encased in a polyethylene glycol hydrogel after a brief exposure to 5 mM tetramisole and before imaging. The immobilized animals were then immersed in 1 × S-Basal solution (100 mM NaCl, 50 mM KPO_4 buffer, 5 μg/ml cholesterol) with 5 mM tetramisole and imaged using a dual inverted selective plane illumination fluorescence microscope (Applied Scientific Instrumentation, USA). Three-dimensional volumetric time-lapse images of the head region were acquired for 10 min for each worm at a rate of 2 volumes/s. The calcium indicator GCaMP6s was used to capture spontaneous *in vivo* neuronal activity throughout the premotor command interneuron circuitry (neuron pairs: AVA, AVB, AVD, AVE, AIB, RIM, and RIV). Postprocessing of imaging data was performed with custom Python and MATLAB (Mathworks, USA) scripts to track the neuronal nuclei in three dimensions in the red fluorescent signal and then to extract the associated green GCaMP6s fluorescence intensities in the surrounding somas.[22] The PVC neurons are located in the tail region and are therefore outside of the imaging volume. The animals were imaged exclusively during early adulthood, because tissue autofluorescence and reduced NLSwCherry expression prohibited reliable neuron tracking in worms aged to late adulthood.

Statistical Methods

Calcium transient onsets (*i.e.*, on transitions) and offsets (*i.e.*, off transitions) captured in AVA *via* confocal microscopy were manually identified by clear shifts in GCaMP6s fluorescence intensity ($\Delta F/F_0$; *i.e.*, the difference in fluorescence above baseline divided by baseline fluorescence), from low to high and high to low, respectively. The duration of each transient was determined by measuring the time difference between the first frame of its on transition and the first frame of the following off transition. The duty ratio, representing the proportion of time that the neuron was in the on state *versus* the off state, was determined by summing all of the calcium transient durations for each recorded fluorescence signal and dividing by the total number of time points in that signal (*i.e.*, 2,400 time points when acquired at 4 frames/s for 10 min).

To examine the manner in which AVA transitions between activity states, individual on and off transitions were manually isolated. Hyperbolic tangent functions fit closely to these activity state transitions and have been used previously to model ion channel currents across biologic membranes.[23,24] Nonlinear fitting of these functions to the activity state transitions eliminates noise and allows for an unbiased assessment of transition properties. The fitted functions were used to calculate the time required to shift from 5% of the maximum value above baseline fluorescence to 95% (rise time) and from 95 to 5% (fall time), respectively.

Average AVA on transition plots were generated by overlaying individual transitions, such that the calculated 5% max($\Delta F/F_0$) positions aligned at the same frame. Average off transition plots were generated in the same manner, with the 95% max($\Delta F/F_0$) positions aligned. Alternatively, average time differential plots of AVA state transitions were generated by overlaying the time derivatives of individual transitions. The time differentials of GCaMP6s fluorescence intensity traces were calculated using total-variation regularization, which suppresses the noise amplification typical of alternative approaches.[25]

Calcium transient onsets (*i.e.*, on transitions) and offsets (*i.e.*, off transitions) captured within the premotor command interneuron circuitry *via* dual inverted selective plane illumination microscopy were identified automatically by convolving the activity trace with a windowing function. The windowing function consists of a square wave with a central null region. By comparing the mean signal intensity before the central null region (*i.e.*, *pre*) with the mean signal intensity after the null region (*i.e.*, *post*), a determination is made as to whether an on transition or an off transition occurred within the central region. If the ratio of *post*:*pre* is greater than 2, then an on transition is determined to have occurred. Conversely, if the ratio *pre*:*post* is greater than 2, then an off transition is determined to have occurred. Based on preliminary data obtained from confocal imaging, a 20-s window with a central null region of 4 s was used to detect on transitions, and a 60-s window with a central null region

of 12 s was used to detect the slower off transitions. After regions that contained on and off transitions were identified, these transitions were fitted with hyperbolic tangent functions as described above, allowing their locations and rapidity to be determined precisely. Transitions whose duration exceeded the permitted maximum specified by the fitting parameters were rejected as outliers. No more than three outliers were found for any particular condition, and in total only 20 of 9,936 events considered were rejected as outliers (0.20%). All other data discussed in this paper were evaluated for outliers, but no further action was necessary. All other data generated/extracted were used, and no data were missing or reconstructed.

Comparisons between measurements were made using a 2 × 5 ANOVA, in which the groups were *condition* (control *vs.* isoflurane) and *genotype/drug* (wild type, *daf-2*, *daf-16*, *ced-3*, rapamycin). ANOVA was applied independently to the rise times and fall times to determine whether there was a detectable difference in means based upon the interaction of *condition* × *genotype/drug*. On rejecting the ANOVA null hypothesis that the measurements were samples of the same parent population, unpaired two-tailed *t* tests were then used to compare the means of the separate experimental configurations. Twelve such tests (m = 12) were performed separately on the rise time and fall time data, respectively. These tests were:

Tests 1 to 4: Comparison of the means of each of the genotypes/drug *daf-2*, *daf-16*, *ced-3*, and rapamycin dependent on *condition* (control *vs.* isoflurane).
Tests 5 to 8: Comparison of the control wild-type mean to the control mean of each of the genotypes/drug *daf-2*, *daf-16*, *ced-3*, and rapamycin.
Tests 9 to 12: Comparison of the isoflurane-exposed wild-type mean to the isoflurane-exposed mean of each of the genotypes/drug *daf-2*, *daf-16*, *ced-3*, and rapamycin.

The significance of the ANOVAs was assessed at $\alpha = 0.05$. Although any individual test at $P < 0.05$ can be significant, performing multiple tests of significance raises the concern that some apparently significant outcomes may be generated by chance, and therefore the further tests under multiple comparisons were performed both at $\alpha = 0.05$ and also using the Bonferroni correction[26] at $\alpha = 0.05/m$ to identify a subset of results of extraordinarily robust significance. The Bonferroni correction is the most conservative test of significance and stipulates such a low α that the likelihood of even one significant value occurring by chance is less than 0.05. However, because the Bonferroni correction requires such a conservative α, it often leads adversely to frequent type II errors in which true discoveries are erroneously rejected. Nevertheless, 8 of the 13 significant results that were found at $\alpha = 0.05$ remained so even under this stringent correction.

All data are reported in the text as the means ± SD. The figures display both the standard deviations of the data and also the 95% CI. We visualized and reviewed the histograms of the underlying distributions, and distributions consistent with the preconditions of the parametric *t* test were observed. All stated *P* values were calculated using the unpaired two-tailed *t* test. Whenever data asymmetries were observed, the nonparametric Mann–Whitney U test was further applied to confirm the validity of the *t* test derived *P* value. No gross disparities between such *P* values were observed. Sample sizes for all experiments were based on prior experience with the experimental designs rather than *a priori* statistical power calculations. All statistical methods were performed using custom scripts and/or functions supported by MATLAB R2017B (Mathworks).

Results

Behavioral Results

Freely moving isoflurane-exposed animals locomoted *via* sinusoidal undulation, primarily in a forward direction with intermittent intervals of backward movement (reversals; fig. 1A), as is typical of wild-type behavior. No differences were observed in the ability of nematodes to respond to aversive mechanical stimuli, indicating that their sensory response remained grossly intact after isoflurane exposure. An eyelash drawn across the anterior portion of the body was similarly likely to yield a reversal response in both isoflurane-exposed and control worms (% response: untreated early adulthood, 94 ± 11, *vs.* isoflurane-exposed early adulthood, 91 ± 13; untreated late adulthood, 65 ± 29, *vs.* isoflurane-exposed late adulthood, 59 ± 28; $P = 0.287$ and 0.248, respectively; fig. 1B). However, the rate at which the worms spontaneously initiated backward movement while locomoting in a food-free environment was reduced in isoflurane-exposed animals. This behavioral shift persisted in both early and late adulthood (reversals/min: untreated early adulthood, 1.14 ± 0.42, *vs.* isoflurane-exposed early adulthood, 0.83 ± 0.55; untreated late adulthood, 1.75 ± 0.64, *vs.* isoflurane-exposed late adulthood, 1.14 ± 0.68; $P = 0.001$ and 0.006, respectively; fig. 1C).

Single Neuron Imaging

Employing the genetically encoded calcium indicator GCaMP6s expressed in a select neuronal subset, we measured the spontaneous activity of the AVA interneuron in both control and isoflurane-exposed animals by measuring its GCaMP6s fluorescence intensity using a confocal microscope (fig. 2A). The AVA interneuron is a key component of the circuitry that mediates the animal's crawling state, displaying little activity during forward crawling but becoming activated during reversals.[17,18]

The activity of the AVA neuron displayed clear and rapid transitions between two discrete states in both the control animals and those that had been exposed to isoflurane at the L1 larval stage. The system rapidly transitions between the forward-moving state, in which AVA is "off" and the

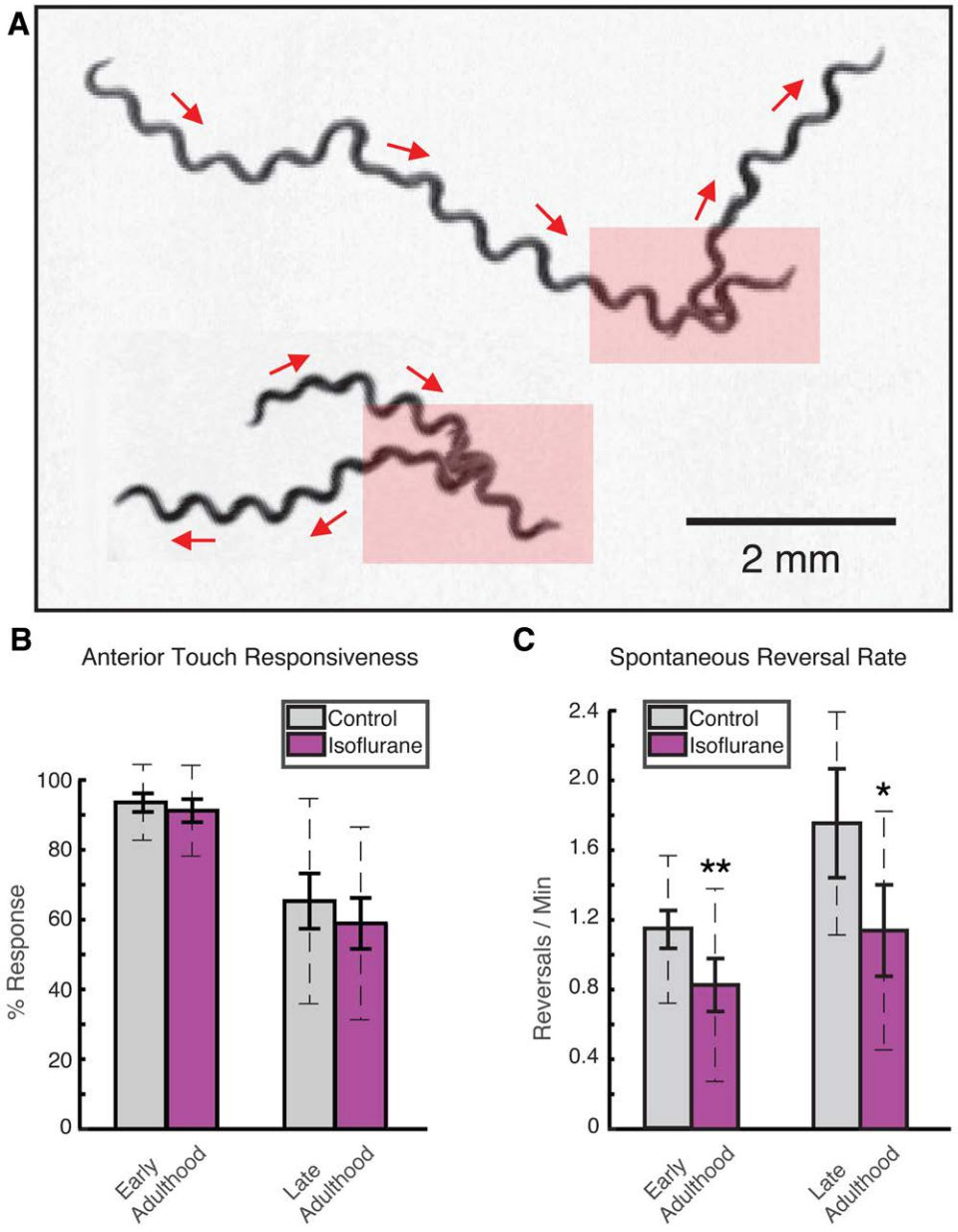

Fig. 1. Assessment of reversal behavior in *C. elegans* after exposure to isoflurane during the first larval stage. (*A*) Travel paths of two unexposed worms initiating spontaneous reversals (*red boxes*), each preceding a shift in path direction. *Red arrows* denote the direction of travel. (*B*) Anterior touch responsiveness in isoflurane-exposed *versus* control worms (isoflurane-exposed early and late adulthood n = 59 and 55, respectively, and control early and late adulthood n = 56 and 53, respectively). The graph displays average response frequencies in individual animals, based on how often an eyelash drawn across the anterior portion of their body elicited a reversal (see Behavioral Assays). (*C*) Spontaneous reversal frequencies of isoflurane-exposed *versus* control worms in an environment devoid of food (isoflurane-exposed early and late adulthood n = 51 and 26, respectively, and control early and late adulthood n = 58 and 16, respectively). *Solid error bars* denote 95% CI, and *dashed error bars* show the SD. **P* < 0.05; ***P* < 0.01, unpaired two-tailed *t* test.

GCaMP signal is low, and the reversal state, in which AVA is "on" and the GCaMP signal is high (illustrated in fig. 2B). We found no change in the relative time spent in either state (*i.e.*, the duty ratio was unchanged, 0.46 ± 0.22 *vs.* 0.42 ± 0.19 for controls; $P = 0.517$), nor the duration in which it stayed in a particular state. The average forward (*i.e.*, off) state duration was 39 ± 77 *vs.* 40 ± 70 s ($P = 0.987$), and the average reversal (*i.e.*, on) state duration was 23 ± 15 *vs.* 23

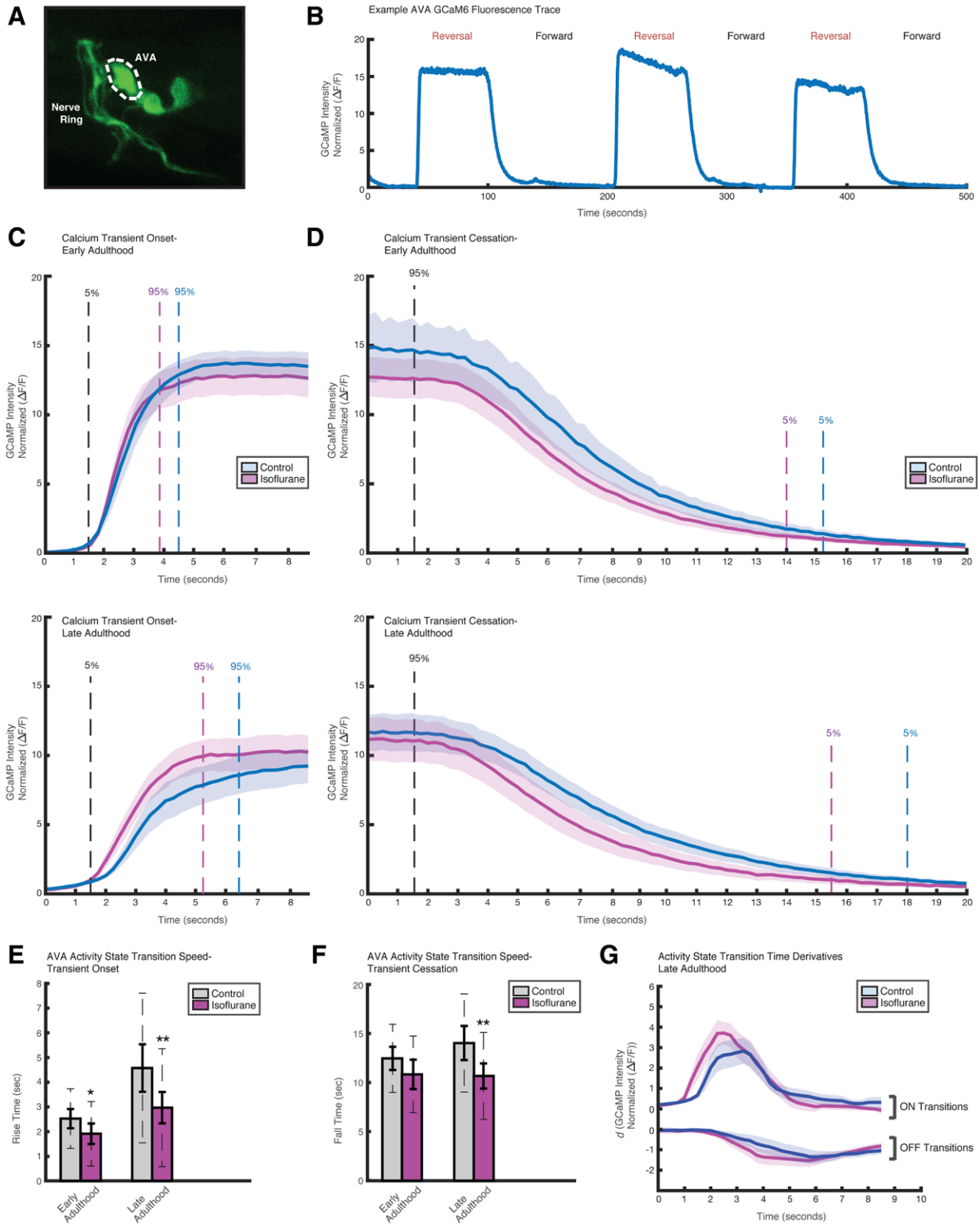

Fig. 2. *In vivo* imaging of spontaneous AVA activity state transitions. (*A*) The command interneuron AVA is readily identifiable in the transgenic *C. elegans* strain QW1574 *via* selective expression of the calcium-sensitive green fluorescent protein GCaMP6s. (*B*) Calcium transients measured from the AVA neuron, captured as intensifications of cytoplasmic GCaMP fluorescence, are indicative of the neuron's innate activity. (*C*, *D*) An increase in AVA fluorescence corresponds with a behavioral reversal event and is reflective of the activity state of the (*Continued*)

± 17 s; $P = 0.733$. This neuronal behavior is consistent with that reported for unanesthetized *C. elegans*, as compared with animals under isoflurane anesthesia.[19] These results demonstrate that the exposed animals had grossly recovered from their anesthetic as expected.

To examine more closely the manner in which AVA transitions between activity states, average traces were calculated for on and off transitions. Individual AVA on transitions (fig. 2C), indicated by clear changes from low to high fluorescence signals, were identified within the measured GCaMP trace for each trial, overlaid, and averaged (see Statistical Methods). Likewise, AVA off transitions (fig. 2D) were averaged at points indicated by clear changes from high to low fluorescence signals. The resultant plots for isoflurane-treated and untreated animals are divergent, with AVA transitions between states more rapid in animals with isoflurane exposure. Moreover, these effects become more pronounced with age: a larger divergence in AVA transition is seen in late adulthood in the 9-day-old animals.

The changes in AVA transition rates were quantified by fitting hyperbolic tangent functions to each state transition observed in the individual trials and calculating the average rise times and fall times for on and off transitions, respectively (see Statistical Methods). In isoflurane-exposed animals, the average AVA rise time was found to be shorter. This effect persisted in both early (1.9 ± 1.3 *vs.* 2.5 ± 1.2 s for controls; $P = 0.028$) and late adulthood (3.0 ± 2.4 *vs.* 4.6 ± 3.0 s; $P = 0.008$), with the difference between control and isoflurane-exposed animals becoming larger and more statistically significant later in life (fig. 2E). Comparably, the average fall time was found to be shorter during late adulthood (10.7 ± 4.3 *vs.* 14.1 ± 4.4 s; $P = 0.001$), following a nonstatistically significant trend in the same direction observed during early adulthood (10.9 ± 3.4 *vs.* 12.5 ± 2.9 s; $P = 0.137$; fig. 2F).

In further analysis, the time differentials of the individual AVA on and off state transitions observed during late adulthood were calculated (see Statistical Methods). These traces were overlaid and averaged, and the resultant plots are again clearly divergent. Traces derived from isoflurane-exposed animals reach a peak amplitude that is greater in magnitude (in both positive and negative transition rates) and also reach this peak more quickly than unexposed animals (fig. 2G). These traces demonstrate a faster and earlier rate of change of intracellular calcium concentration, as measured by GCaMP fluorescence, in animals exposed to isoflurane at the L1 larval stage compared with controls.

Fig. 2. *(Continued)* neuronal network mediating forward and backward movement as indicated. Individual calcium transient onset, "on" (*C*), and cessation, "off" (*D*), fluorescence traces of on and off transitions were overlaid and averaged (see Statistical Methods; *shaded areas* delineate the 95% CI). Hyperbolic tangent functions were fit to these respective on and off transitions and used to calculate the times at which the average traces reach the 5 and 95% fluorescent levels indicated by *dashed lines* (percentages are compared with the maximum value above baseline fluorescence, max($\Delta F/F_0$)). (*E*, *F*) Hyperbolic tangent functions were also fitted to individual calcium transient onset and cessation fluorescence traces and used to calculate the average time required to shift from 5% of the maximum value above baseline fluorescence to 95% (rise time, *E*) and from 95 to 5% (fall time; *F*) respectively (*solid error bars* denote 95% CI, and *dashed error bars* show the SD). (*G*) The time derivatives of AVA activity state transitions were further calculated. Individual calcium transient onset and cessation fluorescence traces, acquired from worms during late adulthood, were differentiated, overlaid, and averaged (see Statistical Methods; *shaded areas* delineate the 95% CI; for onset transitions, isoflurane-exposed early and late adulthood n = 38 and 53 traces from 20 animals each, respectively, and control early and late adulthood n = 37 and 38 traces from 20 and 16 animals, respectively; for cessation transitions, isoflurane-exposed early and late adulthood n = 26 and 46 traces from 19 animals each, respectively, and control early and late adulthood n = 33 and 32 traces from 20 and 14 animals, respectively). *$P < 0.05$; **$P < 0.01$, unpaired two-tailed *t* test.

Multineuron Imaging

To determine whether the postexposure effects on AVA state transition speed are grossly observed throughout the circuitry underlying locomotion, we employed dual inverted selective plane illumination microscopy to capture spontaneous GCaMP fluorescence and, by proxy, the neuron activity within 7 pairs of premotor command interneurons. These 14 neurons (including the anatomical left and right AVA) are centrally involved in locomotive and reversal behavior[17,27] (fig. 3, A and B; see Light-sheet Imaging). Activity traces were extracted from all 14 neurons within each movie, their transitions between states (*i.e.*, rise: off to on; and fall: on to off) were identified, and the average rise and fall times were calculated (see Statistical Methods). In total, 40 movies per condition yielded 560 neuron traces each, from which ~1,050 on events and ~450 off events were extracted. As was the case with AVA alone, the average rise time observed across these interneurons was shorter in isoflurane-exposed young adult animals (3.2 ± 2.0 *vs.* 3.4 ± 2.5 s for controls; $P = 0.030$), whereas the fall time was unchanged (12.9 ± 6.0 *vs.* 12.6 ± 5.6 s for controls; $P = 0.326$; fig. 3, C and D).

In recent behavioral genetics studies, Morgan, Sedensky, and colleagues[10,29] identified molecular modulators of the chemotaxis deficits that follow developmental anesthetic exposure in *C. elegans.* Key among these are genes within the apoptosis cell death pathway, the *daf-2*–dependent stress-response pathway, and the mechanistic Target of Rapamycin (mTOR). Command interneuron state transition speeds were therefore captured and analyzed, as above, in animals harboring specific loss-of-function mutations within *ced-3*, the primary executioner caspase within the *C. elegans* apoptosis pathway; *daf-2*, the *C. elegans* insulin/insulin-like growth factor 1 receptor ortholog; or *daf-16*, the FoxO transcription factor (nuclear translocation of which is negatively regulated by *daf-2*).[30] Worms that had been maintained on the mTOR

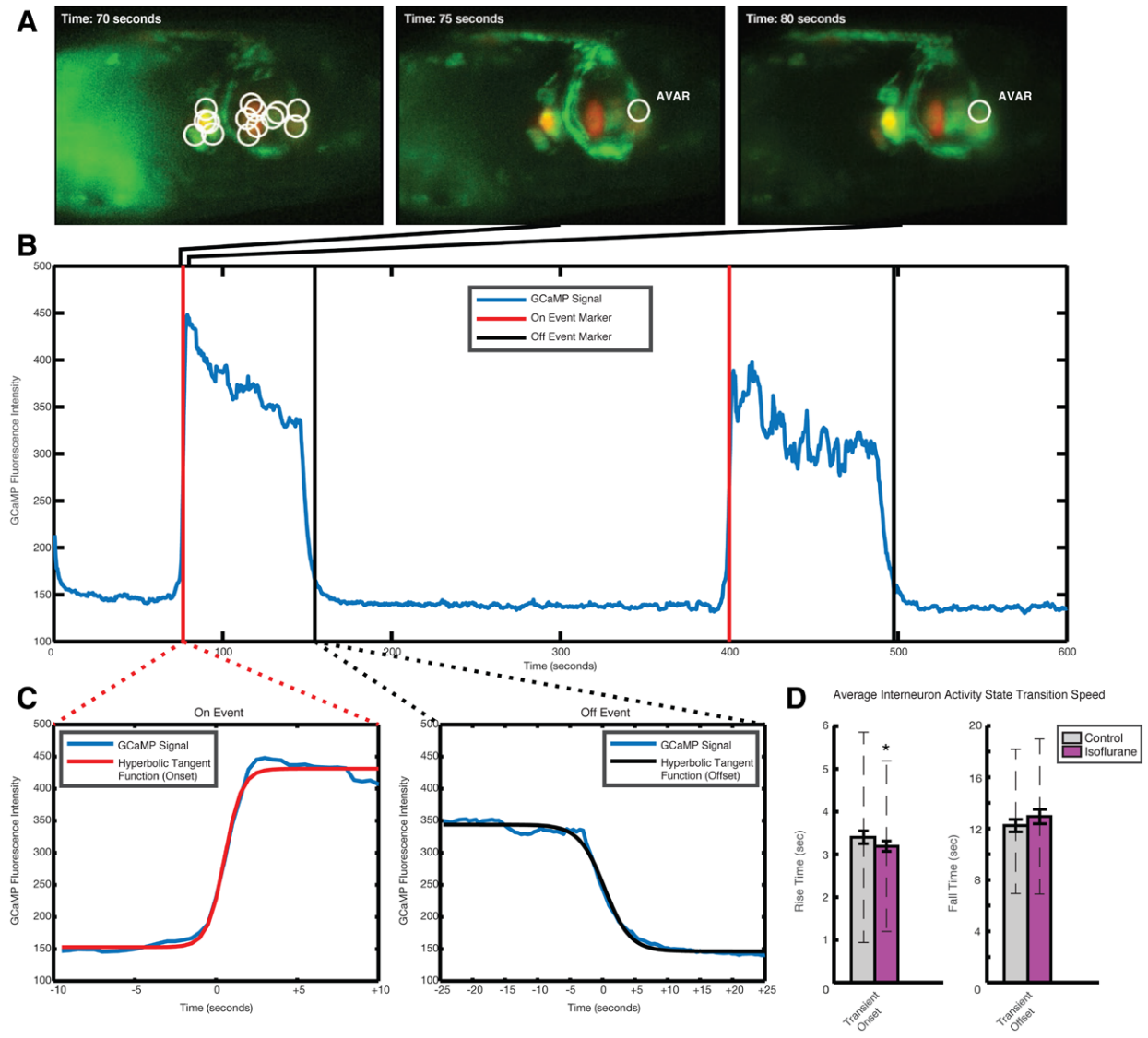

Fig. 3. *In vivo* imaging of spontaneous premotor interneuron activity state transitions. Three-dimensional volumetric time-lapse images of the head region were acquired in the transgenic *C. elegans* strain QW1574 during early adulthood using dual inverted selective plane illumination microscopy. Displayed in (*A*) are maximum intensity projections[28] of volumetric data sets at three consecutive time points, showcasing GCaMP6s expression in seven pairs of premotor interneurons that are centrally involved in locomotive and reversal behavior (AVA, AVB, AVD, AVE, AIB, RIM, and RIV).[17,27] The neurons were identified and tracked *via* nuclear red fluorescent protein NLSwCherry expression, and their GCaMP signals were subsequently extracted (see Light-sheet Imaging). The anatomical right AVA is *circled* in the second and third panels of (*A*), with its GCaMP fluorescence intensity over a 10-min period displayed in (*B*). Using custom MATLAB scripts, which identified substantial shifts in fluorescence intensity (*red* and *black vertical lines*), individual calcium transient onsets and offsets were automatically extracted from these 14 interneurons and fitted to hyperbolic tangent functions (*C*; see Statistical Methods). For each tangent function, the scripts then calculated the rise or fall time. These average values are plotted in (*D*) for control animals and those that had been exposed to isoflurane during the first larval stage (for on transitions: isoflurane-exposed and control early adulthood n = 1,049 and 1,032 traces from 40 animals each, respectively; for off transitions: isoflurane-exposed and control early adulthood n = 441 and 471 traces from 40 animals each, respectively). *Solid error bars* denote 95% CI, and *dashed error bars* show the SD. *$P < 0.05$ unpaired two-tailed *t* test.

inhibitor rapamycin were also examined (see Anesthesia Methods). The results described below are summarized in figure 4 and table 1. The 2 × 5 ANOVA for the difference in means (as described under Statistical Methods) was significant for both the rise and fall times ($P < 0.001$ and $P = 0.009$, respectively). In *ced-3* animals, the postexposure effects on interneuron rise and fall times mirrored those observed in worms with a wild-type background. The average

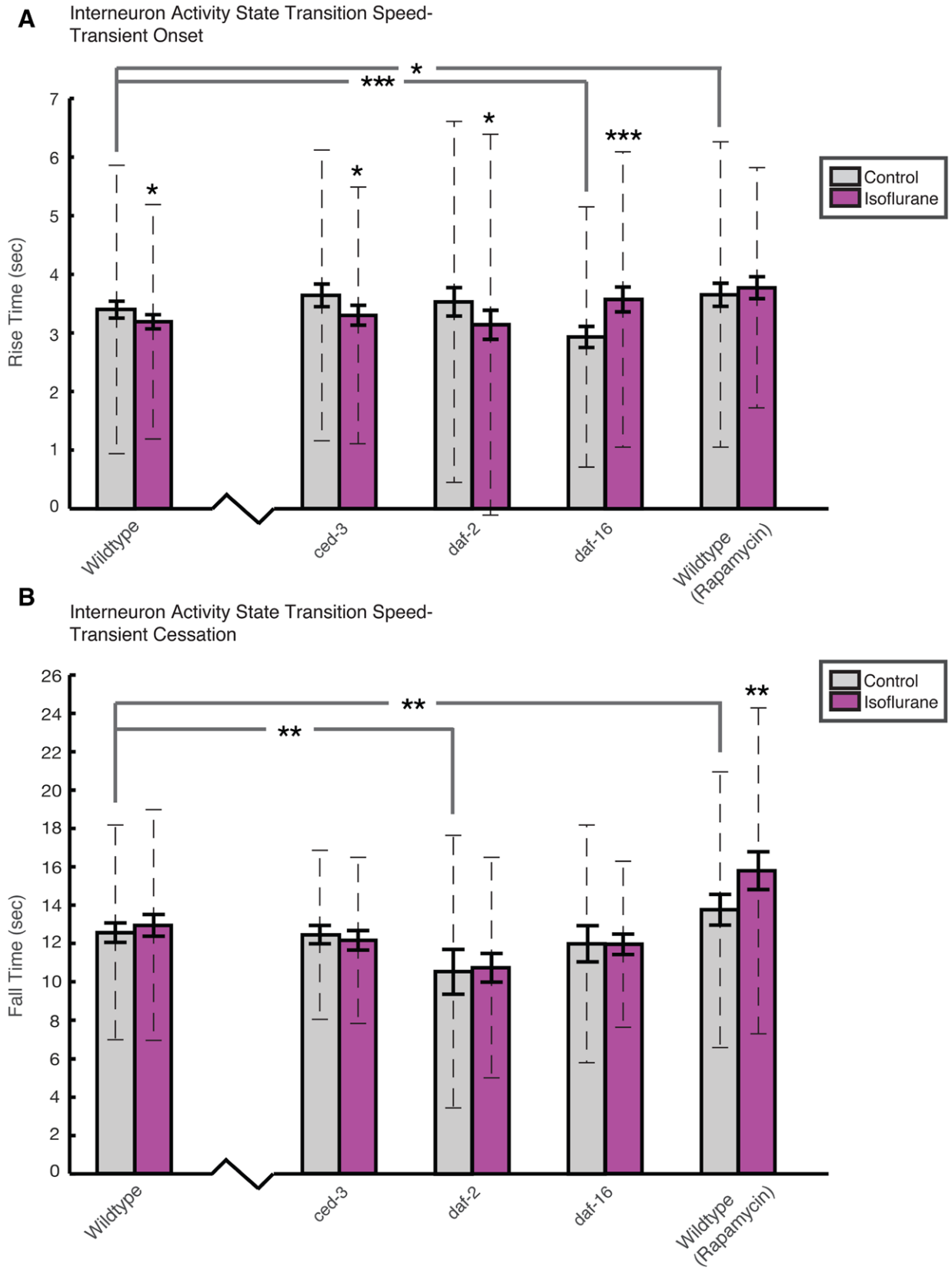

Fig. 4. Modulators of the isoflurane-induced effects on premotor interneuron activity dynamics. After larval exposure to isoflurane, spontaneous interneuron activity state transition speeds were quantified in young adult QW1574 strain worms harboring a loss-of-function mutation in (*Continued*)

rise time was shorter (3.3 ± 2.2 *vs.* 3.6 ± 2.5 s for controls; $P = 0.010$), whereas the fall time was unchanged (12.2 ± 4.3 *vs.* 12.5 ± 4.4 s for controls; $P = 0.408$). These effects were also mirrored in *daf-2* worms, which displayed a shorter rise time (3.1 ± 3.3 *vs.* 3.5 ± 3.1 s for controls; $P = 0.030$) and unchanged fall time (10.7 ± 5.7 *vs.* 10.5 ± 7.1 s for controls; $P = 0.762$). However, in *daf-16* animals, although the fall time remained similarly unchanged in the isoflurane-treated group (12.0 ± 4.3 *vs.* 12.0 ± 6.2 s for controls; $P = 0.966$), the rise time, conversely, lengthened (3.6 ± 2.5 *vs.* 2.9 ± 2.2 s for controls; $P < 0.001$). The postexposure effects on both rise and fall times were also modified in animals that had been maintained on rapamycin. In this case, the Rise Time remained unchanged (3.8 ± 2.1 *vs.* 3.7 ± 2.6 s for controls; $P = 0.401$), whereas the fall time lengthened (15.8 ± 8.5 *vs.* 13.8 ± 7.2 s for controls; $P = 0.002$). In the absence of anesthetic exposure, statistically significant differences in command interneuron state transition speeds were also observed between genotypes. Notably, *daf-2* animals displayed shorter fall times (10.5 ± 7.1 *vs.* 12.6 ± 5.6 s for wild-type; $P < 0.001$), whereas *daf-16* animals displayed shorter Rise Times (2.9 ± 2.2 *vs.* 3.4 ± 2.5 s for wild type; $P < 0.001$). Rapamycin-treated animals displayed both lengthened rise times (3.7 ± 2.6 *vs.* 3.4 ± 2.5 s for wild type; $P = 0.044$) and fall times (13.8 ± 7.2 *vs.* 12.6 ± 5.6 s for wild type; $P = 0.009$).

Discussion

This study demonstrates that exposure of *C. elegans* to isoflurane during the L1 larval development stage fundamentally alters interneuron dynamics and circuit function within the nervous system throughout the animal's lifetime. We measured both the attenuation of the nematode's spontaneous reversal behavior (fig. 1) and altered dynamics of the interneurons mediating this behavior (figs. 2 and 3).

Our findings indicate a neuronal correlate to the chemotaxis deficits previously described by Gentry *et al.*[10] in *C. elegans* after developmental anesthetic exposure. Efficient nematode chemotaxis is dependent upon the stochastic nature of the animal's locomotion. Spontaneous randomized changes in the animal's direction of movement (pirouettes) facilitate its dispersion throughout its environment. Spontaneous reversals constitute a key element of this behavioral strategy by initiating these pirouettes.[15,16] A reduction in spontaneous reversal frequency, as observed in isoflurane-exposed worms, would therefore be expected to hinder the animal's ability to efficiently chemotax, providing a causative link with the findings of Gentry *et al.*[10]

Furthermore, this study provides insight into the effects of isoflurane exposure during neurodevelopment on neuronal function. The command interneurons that we measure here constitute the key neuronal circuitry modulating crawling behavior. This system is comprised of two groups of premotor interneurons that mediate forward (AVB and PVC) and backward (AVA, AVD, and AVE) crawling movement, and an antecedent group of command premotor neurons (AIB, RIM, and RIV) involved in navigation and orientation of the head.[17,27] Although worms will alter movement direction in response to sensory stimuli, they also do so spontaneously. These intermittent changes in movement are facilitated by the command interneuron circuitry that creates spontaneous bimodal activity patterns, consisting of either forward or reverse crawling states.[18] The behavioral deficits in anesthetic-exposed animals will ultimately depend on the activity within this simple well characterized command circuitry. Measuring activity of the AVA command interneuron, we observe a distinct increase in the neuronal transition rate from an off to an on state, which corresponds to a transition from the forward to backward crawling state (fig. 2, C and E). Expanding these measurements to additional command premotor neurons in the animal's head (AVA, AVB, AVD, AVE, AIB, RIM, and RIV) and automating the activity analysis, we confirm an increase in the off to the on state transition rate in isoflurane-exposed animals across the command motor neuron circuitry (fig. 3). It is further remarkable that the effect of isoflurane exposure on neuronal activity is an *increase* in transition speed rather than the decrease that one might expect from generalized degradation. Regardless, these alterations in neuronal activity indicate a fundamental shift in the behavioral state dynamics of the system at large and are congruent with the disruption of crawling behavior observed here and previously.[18]

To gain insight into the cellular mechanisms underlying the alteration in neuronal activity, we measured command neuron dynamics in animals with abolished functionality in specific proteins previously implicated in anesthesia-induced neurotoxicity. CED-3 is the primary executioner caspase

Fig. 4. *(Continued)* the apoptotic executioner caspase *ced-3*, the insulin/insulin-like growth factor 1 receptor ortholog *daf-2*, or the FoxO transcription factor *daf-16*. Alternatively, animals with a wild-type background were grown on plates containing rapamycin, the mechanistic Target of Rapamycin (mTOR) inhibitor. The results were then compared with those previously acquired in animals with a wild-type background (fig. 3D). The average interneuron rise times and fall times are plotted in (*A*) and (*B*), respectively (see Statistical Methods). For each condition, 20 animals were used, except for the wild-type conditions, for which 40 animals were used (for on transitions (*A*): wild-type isoflurane-exposed and control n = 1,049 and 1,032 traces, *ced-3* isoflurane-exposed and control n = 645 and 633 traces, *daf-2* isoflurane-exposed and control n = 651 and 620 traces, *daf-16* isoflurane-exposed and control n = 543 and 588 traces, and rapamycin isoflurane-exposed and control n = 460 and 673 traces, respectively; for off transitions (*B*): wild-type isoflurane-exposed and control n = 441 and 471 traces, *ced-3* isoflurane-exposed and control n = 280 and 329 traces, *daf-2* isoflurane-exposed and control n = 229 and 141 traces, *daf-16* isoflurane-exposed and control n = 254 and 279 traces, and rapamycin isoflurane-exposed and control n = 287 and 311 traces, respectively). *Solid error bars* denote 95% CI, and *dashed error bars* show the SD. *$P < 0.05$; **$P < 0.01$; ***$P < 0.001$, unpaired two-tailed *t* test.

Table 1. Average Rise and Fall Times of Spontaneous Calcium Transients

Genotype/Drug	Condition	Rise Time, s	Traces	Significance: Comparison with Control Condition		Significance: Comparison with Wild-type Genotype	
Rise times							
Wild-type	Control	3.4 ± 2.5	n = 1,032	$P = 0.030$	*		
	Isoflurane	3.2 ± 2.0	n = 1,049				
ced-3	Control	3.6 ± 2.5	n = 633	$P = 0.010$	*	$P = 0.058$	
	Isoflurane	3.3 ± 2.2	n = 645			$P = 0.277$	
daf-2	Control	3.5 ± 3.1	n = 620	$P = 0.030$	*	$P = 0.351$	
	Isoflurane	3.1 ± 3.3	n = 651			$P = 0.731$	
daf-16	Control	2.9 ± 2.2	n = 588	$P < 0.001$	†	$P < 0.001$	†
	Isoflurane	3.6 ± 2.5	n = 543			$P < 0.001$	†
Rapamycin	Control	3.7 ± 2.6	n = 673	$P = 0.401$		$P = 0.044$	*
	Isoflurane	3.8 ± 2.1	n = 460			$P < 0.001$	†
Fall times							
Wild-type	Control	12.6 ± 5.6	n = 471	$P = 0.326$			
	Isoflurane	12.9 ± 6.0	n = 441				
ced-3	Control	12.5 ± 4.4	n = 329	$P = 0.408$		$P = 0.768$	
	Isoflurane	12.2 ± 4.3	n = 280			$P = 0.060$	
daf-2	Control	10.5 ± 7.1	n = 141	$P = 0.762$		$P < 0.001$	†
	Isoflurane	10.7 ± 5.7	n = 229			$P < 0.001$	†
daf-16	Control	12.0 ± 6.2	n = 279	$P = 0.966$		$P = 0.192$	
	Isoflurane	12.0 ± 4.3	n = 254			$P = 0.024$	*
Rapamycin	Control	13.8 ± 7.2	n = 311	$P = 0.002$	†	$P = 0.009$	*
	Isoflurane	15.8 ± 8.5	n = 287			$P < 0.001$	†

Shown are the average rise and fall times of spontaneous calcium transients captured from premotor interneurons in young adult *C. elegans* after exposure to isoflurane at the L1 larval stage. Worms harboring null mutations in *ced-3*, *daf-2*, or *daf-16* were examined, as were the animals treated with rapamycin, the mechanistic Target of Rapamycin (mTOR) inhibitor. The effects of isoflurane on interneuron activity state transition speeds were then compared with those previously obtained in wild-type, untreated animals. These data are plotted graphically in figure 4. The data are given as means ± 95% CI (*solid error bars*) and ± SD (*dashed error bars*).

*Individually $P < 0.05$ *via* unpaired two-tailed *t* test. †Significant after Bonferroni multiple comparisons correction (see Statistical Methods).

within the conserved *C. elegans* apoptotic pathway.[31] Although CED-3 activity appears to play a role in the chemotaxis deficit of isoflurane-exposed animals,[10] the *ced-3* null mutation had no effect on the activity dynamics of the command interneurons measured here (fig. 4). Likewise, the null mutation of the *C. elegans daf-2* gene, the homolog of the mammalian insulin/insulin-like growth factor 1 receptor, did not alter the postexposure effects on interneuron activity (fig. 4). This is in contrast to previous behavioral measurements in which *daf-2* null mutants did not display changes in chemotaxis index upon developmental anesthetic exposure.[29] Thus, apoptotic cell death as well as insulin signaling, both of which have previously been implicated in the neurotoxic effects of anesthetic, appear to be independent of the subtle alterations in neuronal function measured here. Reconciliation of this discrepancy likely lies in the relative complexity of *C. elegans* chemotaxis, the efficient undertaking of which is dependent upon various behaviors that contribute to locomotive stochasticity and also upon neurophysiological processes, such as chemosensation. Although apoptotic cell death and insulin signaling appear to be independent of the postexposure effects we observe in interneuron physiology, these pathways may yet be involved in the manifestation of other neurobehavioral effects that hinder chemotaxis.

Importantly, both a null mutation within the FoxO transcription factor *daf-16* and pharmacologic inhibition of mTOR with rapamycin alter the neurologic effects of anesthetic exposure. The *daf-16* null mutation facilitated a novel increase in interneuron rise time after isoflurane exposure, whereas blockage of mTOR activity both abolished the isoflurane-induced effects on interneuron rise time and further facilitated a novel increase in interneuron fall time (fig. 4). These findings are reminiscent of prior work demonstrating blockage of anesthesia-induced chemotaxis deficiency in worms *via* mTOR inhibition.[29] A growing body of literature further describes mTOR-dependent anesthesia-induced effects in neurodevelopmentally immature rodents. Mintz and colleagues[32,33] have demonstrated in mouse models that isoflurane anesthesia is capable of eliciting abnormal dendrite arbor and spine development, pre- and postsynaptic marker expression, and also deficiencies in spatial learning and memory. These effects were all blocked by rapamycin administration. mTOR inhibition *via* rapamycin has also been shown to block other postexposure effects elicited by sevoflurane administration in postnatal mice. Notably, enhanced excitatory synaptic transmission in males, characterized by an upregulation of α-amino-3-hydroxy-5-methyl-4-isoxazolepropionic acid

(AMPA) receptor subunit GluA2 and an increased mEPSC frequency, was found to be dependent upon mTOR activation.[34] Such changes to neuronal ultrastructure and synaptic transmission may well account for the behavioral and neurophysiological effects described here.

Our findings are also consistent with the activation of neuronal stress-response pathways in response to anesthetic exposure, as supported by recent work by Morgan, Sedensky, and colleagues.[29] Indeed, whereas *daf-16* facilitates a protective endoplasmic reticulum stress-response pathway,[35,36] mTOR has also been shown to interact with this same stress-response pathway and others.[37,38] Our results therefore add to a mounting body of evidence suggesting that anesthetization during critical periods of nematode development may impact normal neurodevelopment through pathologic activation of stress-response pathways and subsequently alter neuronal activity. Although the molecular and cellular mechanisms underlying these observations require further investigation, our results demonstrate that alterations in *C. elegans* neuronal function and signaling measured here are consistent with histological findings and behavioral defects found in higher organisms in that they are likely dependent on neuronal stress-response pathways.[39–41]

In totality, this study demonstrates the following:

1. Exposure to isoflurane at a critical developmental stage results in a defect in the spontaneous reversal rate in the adult animal that is congruent with defects in chemotaxis behavior observed previously.[10,29]
2. There is a pathologic alteration in the transition dynamics of the AVA neuron, a key command interneuron controlling the animal's forward and reverse crawling states. This effect is inducible by exposure to isoflurane and absent in controls.
3. These effects on AVA transition dynamics are broadly observed throughout the command interneuron circuitry centrally involved in defining and determining the forward and reverse behavioral crawling states of the animal.
4. The mTOR and FoxO transcription factor *daf-16* modulate these effects on transition dynamics, consonant with prior behavioral studies.[29]

Thus, we have observed a permanent defect in the function of neurons controlling behavior that is induced by anesthetic exposure in a developing animal. Moreover, we have linked these defects to the activation of stress-response pathways also implicated in the histological and behavioral effects seen in higher organisms.[38–40] Given the tractability of *C. elegans* for functional neuronal imaging, its entirely mapped connectome, and suitability for genetic manipulation, this simple but powerful model system can serve as a platform for interrogating these molecular pathways underlying anesthesia-induced dysfunction of neuronal circuits after exposure early in life.

Research Support

Supported by National Institutes of Health (Bethesda, Maryland) grant No. R01 GM121457 and by departmental sources.

Competing Interests

Dr. Connor is a consultant for Teleflex, LLC (Wayne, Pennsylvania) on airway equipment design. This activity is unrelated to the material in this manuscript. The other authors declare no competing interests.

Correspondence

Address correspondence to Dr. Connor: Brigham and Women's Hospital, 75 Francis Street, CWN L1, Boston, Massachusetts 02115. cconnor@bwh.harvard.edu.

References

1. Brambrink AM, Back SA, Riddle A, Gong X, Moravec MD, Dissen GA, Creeley CE, Dikranian KT, Olney JW: Isoflurane-induced apoptosis of oligodendrocytes in the neonatal primate brain. Ann Neurol 2012; 72:525–35
2. Jevtovic-Todorovic V, Hartman RE, Izumi Y, Benshoff ND, Dikranian K, Zorumski CF, Olney JW, Wozniak DF: Early exposure to common anesthetic agents causes widespread neurodegeneration in the developing rat brain and persistent learning deficits. J Neurosci 2003; 23:876–82
3. Alvarado MC, Murphy KL, Baxter MG: Visual recognition memory is impaired in rhesus monkeys repeatedly exposed to sevoflurane in infancy. Br J Anaesth 2017; 119:517–23
4. Coleman K, Robertson ND, Dissen GA, Neuringer MD, Martin LD, Cuzon Carlson VC, Kroenke C, Fair D, Brambrink AM: Isoflurane anesthesia has long-term consequences on motor and behavioral development in infant rhesus macaques. Anesthesiology 2017; 126:74–84
5. Raper J, De Biasio JC, Murphy KL, Alvarado MC, Baxter MG: Persistent alteration in behavioural reactivity to a mild social stressor in rhesus monkeys repeatedly exposed to sevoflurane in infancy. Br J Anaesth 2018; 120:761–7
6. Sun LS, Li G, Miller TL, Salorio C, Byrne MW, Bellinger DC, Ing C, Park R, Radcliffe J, Hays SR, DiMaggio CJ, Cooper TJ, Rauh V, Maxwell LG, Youn A, McGowan FX: Association between a single general anesthesia exposure before age 36 months and neurocognitive outcomes in later childhood. JAMA 2016; 315:2312–20
7. Warner DO, Zaccariello MJ, Katusic SK, Schroeder DR, Hanson AC, Schulte PJ, Buenvenida SL, Gleich SJ, Wilder RT, Sprung J, Hu D, Voigt RG, Paule

MG, Chelonis JJ, Flick RP: Neuropsychological and behavioral outcomes after exposure of young children to procedures requiring general anesthesia: The Mayo Anesthesia Safety in Kids (MASK) study. Anesthesiology 2018; 129:89–105
8. Davidson AJ, Disma N, de Graaff JC, Withington DE, Dorris L, Bell G, Stargatt R, Bellinger DC, Schuster T, Arnup SJ, Hardy P, Hunt RW, Takagi MJ, Giribaldi G, Hartmann PL, Salvo I, Morton NS, von Ungern Sternberg BS, Locatelli BG, Wilton N, Lynn A, Thomas JJ, Polaner D, Bagshaw O, Szmuk P, Absalom AR, Frawley G, Berde C, Ormond GD, Marmor J, McCann ME; GAS consortium: Neurodevelopmental outcome at 2 years of age after general anaesthesia and awake-regional anaesthesia in infancy (GAS): An international multicentre, randomised controlled trial. Lancet 2016; 387:239–50
9. McCann ME, de Graaff JC, Dorris L, Disma N, Withington D, Bell G, Grobler A, Stargatt R, Hunt RW, Sheppard SJ, Marmor J, Giribaldi G, Bellinger DC, Hartmann PL, Hardy P, Frawley G, Izzo F, von Ungern Sternberg BS, Lynn A, Wilton N, Mueller M, Polaner DM, Absalom AR, Szmuk P, Morton N, Berde C, Soriano S, Davidson AJ; GAS Consortium: Neurodevelopmental outcome at 5 years of age after general anaesthesia or awake-regional anaesthesia in infancy (GAS): An international, multicentre, randomised, controlled equivalence trial. Lancet 2019; 393:664–77
10. Gentry KR, Steele LM, Sedensky MM, Morgan PG: Early developmental exposure to volatile anesthetics causes behavioral defects in *Caenorhabditis elegans*. Anesth Analg 2013; 116:185–9
11. Roberts WM, Augustine SB, Lawton KJ, Lindsay TH, Thiele TR, Izquierdo EJ, Faumont S, Lindsay RA, Britton MC, Pokala N, Bargmann CI, Lockery SR: A stochastic neuronal model predicts random search behaviors at multiple spatial scales in C. elegans. Elife 2016; 5:e12572
12. Berg HC: Chemotaxis in bacteria. Annu Rev Biophys Bioeng 1975; 4:119–36
13. Berg HC, Dyson F: Random walks in biology. Phys Today 1987; 40:73–4
14. Pierce-Shimomura JT, Morse TM, Lockery SR: The fundamental role of pirouettes in *Caenorhabditis elegans* chemotaxis. J Neurosci 1999; 19:9557–69
15. Croll NA: Behavioural analysis of nematode movement. Adv Parasitol 1975; 13:71–122
16. Croll NA: Components and patterns in the behaviour of the nematode *Caenorhabditis elegans*. J Zool 1975; 176:159–76
17. Chalfie M, Sulston JE, White JG, Southgate E, Thomson JN, Brenner S: The neural circuit for touch sensitivity in *Caenorhabditis elegans*. J Neurosci 1985; 5:956–64
18. Kawano T, Po MD, Gao S, Leung G, Ryu WS, Zhen M: An imbalancing act: Gap junctions reduce the backward motor circuit activity to bias *C. elegans* for forward locomotion. Neuron 2011; 72:572–86
19. Awal MR, Austin D, Florman J, Alkema M, Gabel CV, Connor CW: Breakdown of neural function under isoflurane anesthesia: *In vivo*, multineuronal imaging in *Caenorhabditis elegans*. Anesthesiology 2018; 129:733–43
20. Rueden CT, Schindelin J, Hiner MC, DeZonia BE, Walter AE, Arena ET, Eliceiri KW: ImageJ2: ImageJ for the next generation of scientific image data. BMC Bioinformatics 2017; 18:529
21. Burnett K, Edsinger E, Albrecht DR: Rapid and gentle hydrogel encapsulation of living organisms enables long-term microscopy over multiple hours. Commun Biol 2018; 1:73
22. Awal M, Wirak G, Gabel C, Connor C: Pan-neuronal tracking of neuronal activity in anesthetized *C. elegans*. Paper presented at Annual Meeting of the International Anesthesia Research Society, Montreal, Canada, May 16–20, 2019
23. Liu Q, Kidd PB, Dobosiewicz M, Bargmann CI: *C. elegans* AWA olfactory neurons fire calcium-mediated all-or-none action potentials. Cell 2018; 175:57–70
24. Rinzel J, Ermentrout GB: Analysis of neural excitability and oscillations, Methods in Neuronal Modeling: From Synapses to Networks. Edited by Koch C, Segev I. Cambridge, Massachusetts, MIT Press, 1989, pp 135–69
25. Chartrand R: Numerical differentiation of noisy, nonsmooth data. ISRN Appl Math 2011; 2011:1–11
26. Bland JM, Altman DG: Multiple significance tests: The Bonferroni method. *BMJ*. 1995; 310:170
27. Gray JM, Hill JJ, Bargmann CI: A circuit for navigation in *Caenorhabditis elegans*. Proc Natl Acad Sci U S A 2005; 102:3184–91
28. Wallis JW, Miller TR: Three-dimensional display in nuclear medicine and radiology. J Nucl Med 1991; 32:534–46
29. Na HS, Brockway NL, Gentry KR, Opheim E, Sedensky MM, Morgan PG: The genetics of isoflurane-induced developmental neurotoxicity. Neurotoxicol Teratol 2017; 60:40–49
30. Henderson ST, Johnson TE: *daf-16* integrates developmental and environmental inputs to mediate aging in the nematode *Caenorhabditis elegans*. Curr Biol 2001; 11:1975–80
31. Ellis HM, Horvitz HR: Genetic control of programmed cell death in the nematode *C. elegans*. Cell 1986; 44:817–29
32. Kang E, Jiang D, Ryu YK, Lim S, Kwak M, Gray CD, Xu M, Choi JH, Junn S, Kim J, Xu J, Schaefer M, Johns RA, Song H, Ming GL, Mintz CD: Early postnatal exposure to isoflurane causes cognitive deficits and

disrupts development of newborn hippocampal neurons via activation of the mTOR pathway. PLoS Biol 2017; 15:e2001246
33. Xu J, Mathena RP, Xu M, Wang Y, Chang C, Fang Y, Zhang P, Mintz CD: Early developmental exposure to general anesthetic agents in primary neuron culture disrupts synapse formation via actions on the mTOR pathway. Int J Mol Sci 2018; 19:E2183
34. Ju X, Ryu MJ, Cui J, Lee Y, Park S, Hong B, Yoo S, Lee WH, Shin YS, Yoon S-H, Kweon GR, Kim YH, Ko Y, Heo JY, Chung W: The mTOR inhibitor rapamycin prevents general anesthesia-induced changes in synaptic transmission and mitochondrial respiration in late postnatal mice. Front Cell Neurosci 2020; 14:4
35. Libina N, Berman JR, Kenyon C: Tissue-specific activities of *C. elegans* DAF-16 in the regulation of lifespan. Cell 2003; 115:489–502
36. Henis-Korenblit S, Zhang P, Hansen M, McCormick M, Lee SJ, Cary M, Kenyon C: Insulin/IGF-1 signaling mutants reprogram ER stress response regulators to promote longevity. Proc Natl Acad Sci U S A 2010; 107:9730–5
37. Endo H, Murata K, Mukai M, Ishikawa O, Inoue M: Activation of insulin-like growth factor signaling induces apoptotic cell death under prolonged hypoxia by enhancing endoplasmic reticulum stress response. Cancer Res 2007; 67:8095–103
38. Reiling JH, Sabatini DM: Stress and mTORture signaling. Oncogene 2006; 25:6373–83
39. Zhu G, Tao L, Wang R, Xue Y, Wang X, Yang S, Sun X, Gao G, Mao Z, Yang Q: Endoplasmic reticulum stress mediates distinct impacts of sevoflurane on different subfields of immature hippocampus. J Neurochem 2017; 142:272–85
40. Chen G, Gong M, Yan M, Zhang X: Sevoflurane induces endoplasmic reticulum stress mediated apoptosis in hippocampal neurons of aging rats. PLoS One 2013; 8:e57870
41. Komita M, Jin H, Aoe T: The effect of endoplasmic reticulum stress on neurotoxicity caused by inhaled anesthetics. Anesth Analg 2013; 117:1197–204